We now compute the limit

$$\Lambda = \oint_L \lim_{\tau_g \to \tau_f} \lim \frac{\frac{d}{d\tau_g}\left(f\frac{\partial g}{\partial \nu} - g\frac{\partial f}{\partial \nu}\right)}{\frac{d}{d\tau_g}(\tau_f^2 - \tau_g^2)}\, dl \tag{34}$$

to get

$$\Lambda = -\frac{1}{2\tau}\oint_L \left(f\frac{\partial^2 g}{\partial\tau\partial\nu} - \frac{\partial g}{\partial\tau}\frac{\partial f}{\partial\nu}\right) dl. \tag{35}$$

Equation (35) can be used to get (11), (26), and (27).

A. TEM–TEM coupling

Equation (21) follows trivially from Green's first identity

$$\iint_{\Omega_s} \nabla_t\psi_{0b}\cdot\nabla_t\psi_{0s}\, d\Omega = -\iint_{\Omega_s} \psi_{0b}\nabla_t^2\psi_{0s}\, d\Omega + \oint_{L_s}\psi_{0b}\frac{\partial\psi_{0s}}{\partial\nu}\, dl$$

since $\nabla_t^2\psi_{0s} = 0$.

B. TM–TEM coupling

Equation (22) follows similarly from Green's first identity.

C. TE–TEM coupling

Using the general result [1]

$$\iint_{\Omega} \nabla_t f\cdot\nabla_t g\times\mathbf{u}_z\, d\Omega = \oint_L f\frac{\partial g}{\partial l}\, dl$$

we can write

$$\langle\mathbf{e}_b^{\mathrm{TE}}, \mathbf{e}_s^{\mathrm{TEM}}\rangle = -\oint_{L_s}\varphi_b\frac{\partial\psi_{0s}}{\partial l}\, dl = 0$$

since ψ_{0s} is constant on L_s.

D. TEM–TM coupling

The integral is

$$\iint_{\Omega_s} \nabla_t\psi_{0b}\cdot\nabla_t\psi_s\, d\Omega = -\iint_{\Omega_s}\psi_s\nabla_t^2\psi_{0b}\, d\Omega + \oint_{L_s}\psi_s\frac{\partial\psi_{0b}}{\partial\nu}\, dl \tag{36}$$

and since $\nabla_t^2\psi_{0b} = 0$ in Ω_s and $\psi_s = 0$ on L_s, the result is zero.

REFERENCES

[1] G. G. Gentili, "Properties of TE–TM mode-matching techniques," *IEEE Trans. Microwave Theory Tech.*, vol. 39, pp. 1669–1672, Sept. 1991.

[2] G. G. Gentili, M. Politi, R. Maffia, G. Macchiarella, and A. Melloni, "Analysis of the discontinuity between a ridged and a rectangular waveguide by an efficient mode-matching technique," in *Proc. Eur. Microwave Conf*, Stuttgart, Germany, 1991, pp. 553–558.

[3] L. Accatino and G. Bertin, "Design of coupling irises between circular cavities by modal analysis," *IEEE Trans. Microwave Theory Tech.*, vol. 42, pp. 1307–1313, July 1994.

[4] F. Arndt, R. Beyer, J. Reiter, T. Sieverding, and T. Wolf, "Automated design of waveguide components using hybrid mode-matching/numerical EM building blocks in optimization-oriented CAD frameworks—State of the art and recent advances," *IEEE Trans. Microwave Theory Tech.*, vol. 45, pp. 747–760, May 1997.

[5] G. Conciauro, M. Guglielmi, and R. Sorrentino, *Advanced Modal Analysis*. New York: Wiley, 1999.

[6] P. Guillot, P. Couffignal, H. Baudrand, and B. Theron, "Improvement in calculation of some surface integrals: Application to junction characterization in cavity filter design," *IEEE Trans. Microwave Theory Tech.*, vol. 41, pp. 2156–2160, Dec. 1993.

[7] T. Itoh, *Numerical Techniques for Microwave and Millimeter-Wave Passive Structures*. New York: Wiley, 1989, pp. 592–621.

Improved Automatic Parameter Extraction of InP-HBT Small-Signal Equivalent Circuits

B. Willén, Marcel Rohner, I. Schnyder, and H. Jäckel

***Abstract*—An improved automatic extraction technique for determination of the element values of an InP heterojunction-bipolar-transistor small-signal T-model is presented. Numerical optimization is shown to yield reproducible and physically relevant results when using a suitable figure-of-merit. The outcome of such an extraction is displayed for a range of operation points and the resulting bias dependencies of the element values is shown to be in good agreement with theoretical effects. The technique is further used to validate the quality of the extraction itself by showing a significant sensitivity to a deliberate error in the value of each element.**

***Index Terms*—HBT, InP, numerical parameter extraction.**

I. INTRODUCTION

Computer-aided design of integrated circuits relies on equivalent transistor models that are able to describe the terminal characteristics of individual devices properly. Element values of such models for InP-based heterojunction bipolar transistors (HBTs) are regularly extracted by fitting simulated S-parameters to measured numerically. Reproducibility, as well as physical relevance of the extracted small-signal model elements, are important prerequisites for process monitoring and device optimization, but it is well known that this extraction represents an overdetermined optimization problem. The frequency range covered by state-of-the-art measurement equipments does not extend to all relevant circuit poles, and lumped-circuit models become questionable at high frequencies. Several methods have been proposed to overcome this nondeterministic behavior as follows.

- Some element values, i.e., the ratio of the internal to external collector area and the resistance of the metal contacts, are taken from the geometrical layout or test structures to reduce the number of elements needed to be extracted. These values should ideally also be derived from the measurements to be able to reveal fabrication deficiencies.
- Most notable are analytical extraction methods where some element values are found by extrapolation rather than numerical optimization, e.g., from $Z_{11} - Z_{12}$, $Z_{22} - Z_{21}$, $Z_{12} - Z_{21}$, and Z_{12} [1]–[3].

By fixing some element values *a priori*, the dimension of the parameter space is decreased so that subsequent tuning becomes better defined.

Manuscript received February 14, 2001.

B. Willén is with the Department of Electronics, Royal Institute of Technology, S-164 40 Kista, Sweden.

M. Rohner, I. Schnyder, and H. Jäckel are with the Electronics Laboratory, Swiss Federal Institute of Technology Zürich, CH-8092 Zürich, Switzerland (e-mail: rohner@ife.ee.ethz.ch).

Publisher Item Identifier S 0018-9480(02)01167-5.

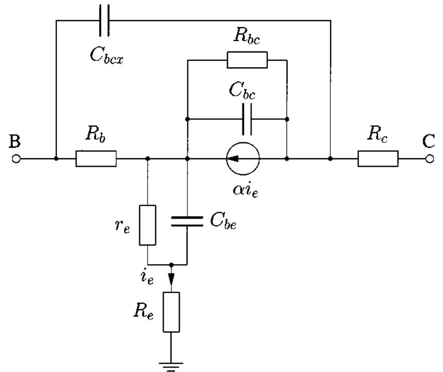

Fig. 1. Small-signal T-model.

We argue here that the same effect can be obtained by a careful choice of the error functions used for numerical optimization.

II. Analysis

In finding the element values of an equivalent circuit, the most basic approach is to fit the output of the model to an RF characterization of a realized device using the figure-of-merit

$$G_{\rm opt} = \min_P \frac{1}{\Delta f} \int_{\Delta f} \sum_k W_k E^2(F_k, F_k^*(P))\, df \tag{1}$$

where F_k and $F_k^*(P)$ are a measured and simulated quantity, respectively, $F_k^*(P)$ depends on the parameter set P of the small-signal circuit, $E(\cdot, \cdot)$ is an error function that is a measure of the deviation between F_k and F_k^*, W_k is a weighting factor that enforce a reasonable distribution of the errors to the different terms, and Δf is the used frequency range. The weighting factors can be used to reduce the relative error of the parameter with the worst fit. In this paper, $W_k = 1$ was employed for all factors.

It is a common, albeit questionable, approach to employ

$$E(F_k, F_k^*) = F_k - F_k^* \qquad \forall\, k \tag{2}$$

where $F(k) = S_{ij}$ or Z_{ij} for $k = 2i + j - 2 = 1 \cdots 4$. The inadequacy of equivalent circuits to exactly reproduce the device behavior, as well as measurement errors, inherently cause a residual error, and the outcome of such an extraction technique offers the same total error for the surface defined by

$$\sum_k W_k E_k^2 = {\rm const} \tag{3}$$

rendering nonreproducible results.

Analytical extraction methods improve on this by introducing

$$F_5' = Z_{11} - Z_{12} \tag{4}$$

$$F_6' = Z_{12} - Z_{21} \tag{5}$$

$$F_7' = Z_{22} - Z_{21} \tag{6}$$

as additional quantities in a limited frequency range. Using (2), this implies that $Z_{ij} - Z_{mn} = Z_{ij}^* - Z_{mn}^*$, which has the effect of minimizing the error along the lines $E(Z_k, Z_k^*) = E(Z_l, Z_l^*)\ (k, l = 1 \ldots 4)$. In doing so, the total remaining error is distributed equally to all Z-parameters. Fixing the Z-parameters this way may affect the fit of the S-parameters since the denominator $D = (Z_{11} + 1)(Z_{22} + 1) - Z_{12}Z_{21}$ used for Z-to-S-conversion is deteriorated by the actual error distribution according to (neglecting higher order terms)

$$D^* - D \approx \epsilon_{22} Z_{11} + \epsilon_{11} Z_{22} - \epsilon_{12} Z_{21} - \epsilon_{21} Z_{12} \tag{7}$$

TABLE I
COMPARISON OF THE EXTRACTION METHODS. PARAMETER VALUES AND INSIGNIFICANCES $P_i \pm S(P_i)$ FOR $I_c = 10$ mA AND $U_{ce} = 2$ V USING Z, S, AND $S + B$ PARAMETERS ARE LISTED

	Z	S	S+B	
	F_1'–F_4'	F_1–F_4	F_1–F_5	
C_{be}	164±210	179 ± 250	210 ± 130	pF
τ	0±2.4[a]	0.46 ± 0.98	0.35 ± 0.51	ps
β_0	74±51	81 ± 90	87 ± 26	1
R_{bi}	32.5±24	24 ± 6.1	24 ± 6.1	Ω
r_e	6.3±7.8	3.8 ± 0.86	3.7 ± 0.90	Ω
R_{cx}	0±25	0 ± 17	0 ± 23	Ω
R_{bc}	23±29	∞[b]	∞[b]	kΩ
C_{bc}	3.9±6.8	10 ± 4.1	9.9 ± 4.2	fF
C_{bcx}	26±8.9	21 ± 5.0	21 ± 5.8	fF

[a] Negative if not limited to positive values.
[b] Insignificane undefined at ∞.

where $\epsilon_{ij} = E(Z_{ij}, Z_{ij}^*)$. Therefore, by assigning all Z-parameters an equal error $\epsilon_{ij} = \epsilon$, the increased reproducibility is gained on cost of accuracy in the S-parameters.

To assess the reproducibility of different extraction techniques, we introduce the parameter insignificance

$$S(P_i) = \sqrt{\frac{2G_{\rm opt}}{d^2 G_{P_i}/dP_i^2}} \tag{8}$$

as a measure of the change in the parameter P_i required to obtain $G'_{P_i} = 2G_{\rm opt}$, where G'_{P_i} is the second-order Taylor expansion of

$$G_{P_i} = \min_{P \setminus P_i} \frac{1}{\Delta f} \int_{\Delta f} \sum_k W_k E^2\Big(F_k, F_k^*(P)\Big)\, df \tag{9}$$

which is the figure-of-merit when changing the parameter P_i and reoptimizing. A large value for the insignificance is equivalent to a low sensitivity to a change in that parameter.

III. Numerical Extraction

The method itself is generic and can be easily adapted to different topologies of small-signal models. The T-model of Fig. 1 was adopted in this study because of its close relation to device physics. The common base current gain is

$$\alpha = \frac{\beta_0}{1 + \beta_0} \frac{e^{-j\omega\tau}}{1 + j\omega r_e C_{be}} \tag{10}$$

where τ is the excess phase delay in addition to the single-pole approximation with $C_{be} = C_{be,diff} + C_{be,depl}$ [4]. Parasitic pad capacitors, as well as interconnect inductors, are assumed to have been deembedded during initial calibration. The model is very sensitive to this and the entire extraction relies on an accurate result. The emitter resistance R_e is the only parameter requiring multibias extraction. Measurements at several collector currents are used to extrapolate R_e from $R_e + r_e$ versus $1/I_c$ [5]. The $R_e + r_e$ is extracted analytically from ${\rm Re}(Z_{12})$ to save CPU time since numerical extraction would require a second optimization. In doing so, an error of less than 0.2 Ω was found for R_e, causing a change of less than 5% in the other elements.

After this step, nine elements remain to be determined. They are tuned by gradient optimization to minimize the figure-of-merit $G_{\rm opt}$, described in the previous section. Instead of $E(\cdot, \cdot)$ in (2), we use a

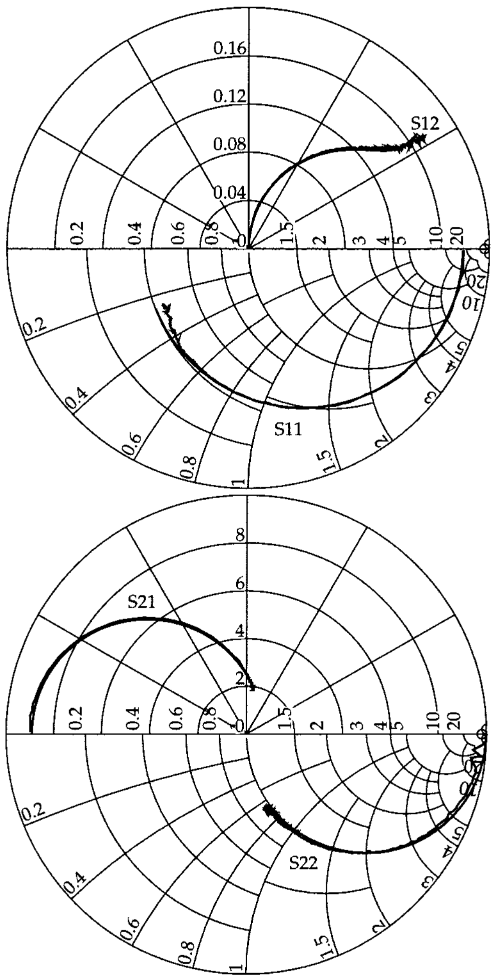

Fig. 2. Comparison between the measured and modeled S-parameters.

relative error E_M for the magnitude and an absolute error E_P for the phase according to

$$E_M(F_k,\ F_k^*) = \left| \frac{|F_k^*|}{|F_k|} - \frac{|F_k|}{|F_k^*|} \right|^{1/2} \qquad \forall\, k \tag{11}$$

and

$$E_P(F_k,\ F_k^*) = |\angle F_k^* - \angle F_k| \qquad \forall\, k. \tag{12}$$

Here, E_M is designed symmetrically so that errors $F_k^* \ll F_k$ and $F_k^* \gg F_k$ are equally emphasized. The sum in (1) is modified to account for both error functions

$$\sum_k W_{k,\,M} E_M^2 + W_{k,\,P} E_P^2. \tag{13}$$

The method has been tested on a variety of InP-based single- and double-heterojunction devices, both from the Swiss Federal Institute of Technology Zürich, Zürich, Switzerland, and the Royal Institute of Technology, Kista, Sweden. Typical remaining errors in the magnitude of the fitted parameters (S or Z) were less than 5%, and less than 1° in the phase.

IV. Results and Discussion

We present some results gained from a 1.2 × 8 μm InP double heterostructure bipolar transistor (DHBT) [6]. It was evaluated with a collector current in the range of 1–12 mA and with a collector voltage ranging from 1.0 to 3.0 V. The device was measured from 1 to 40 GHz,

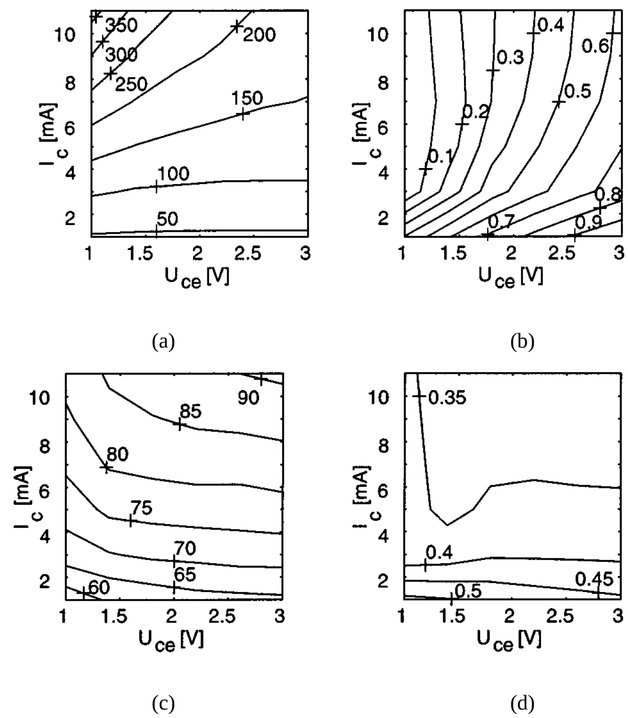

Fig. 3. Extracted bias dependence of some small-signal parameters when including the F_5 term, clearly reproducing the expected behavior. (a) C_{be} [fF]. (b) τ [ps]. (c) β_0. (d) $x = C_{bc}/(C_{bc} + C_{bcx})$.

with an extrapolated maximum oscillation frequency $f_{\max} = 150$ GHz and transit frequency $f_t = 150$ GHz. During calibration, the reference plane was moved forward from the probe tips to the end of the interconnects using a set of dummy pads. The capacitances of these structures were characterized and the resulting Y-parameters automatically subtracted during subsequent device characterization. Empirically, this procedure results in a remaining interconnect impedance and pad capacitance of less than 1 pH and 0.5 fF, respectively.

Insignificances obtained when optimizing for Z-parameters only, i.e., $F_k = Z_{ij}$ $(k = 2i + j - 2)$ are listed in Table I. These values can be used to evaluate the significance of an element value achieved by analytic extraction. From the second column, it is evident that using S-parameters, i.e., $F_k = S_{ij}$ $(k = 2i + j - 2)$, improves the sensitivity of the extraction considerably, as compared with using Z-parameters. The major weakness is in finding the values of three specific elements C_{be} and τ, which can be traded in the low-frequency limit, and β_0, being of importance at low frequencies only. The expression $B = (Z_{12} - Z_{21})/(Z_{22} - Z_{12})$, often used to find the current gain $\beta_0 = B|_{f=0}$, depends critically on the C_{be}-to-τ distribution at high frequencies, as well as the value of β_0 at low frequencies, so that we require

$$F_5 = B \tag{14}$$

to improve on these elements (see Table I). Fig. 2 shows the modeled and measured S-parameters at a typical operating point. The bias dependence of some of the critical circuit parameters are shown in Fig. 3. Comparing the contour plots of Fig. 4, it is seen that the insignificance is considerably reduced over the entire bias range when including F_5. R_{bc} of this device is too high to have any effect. The magnitude of the extracted elements shown in Fig. 3 is consistent with the expected device behavior. Both physically relevant values and improved reproducibility may thus be obtained by introducing F_5. The advantages of the new method also manifests in an improved convergence rate of the optimization because of the increased sensitivity.

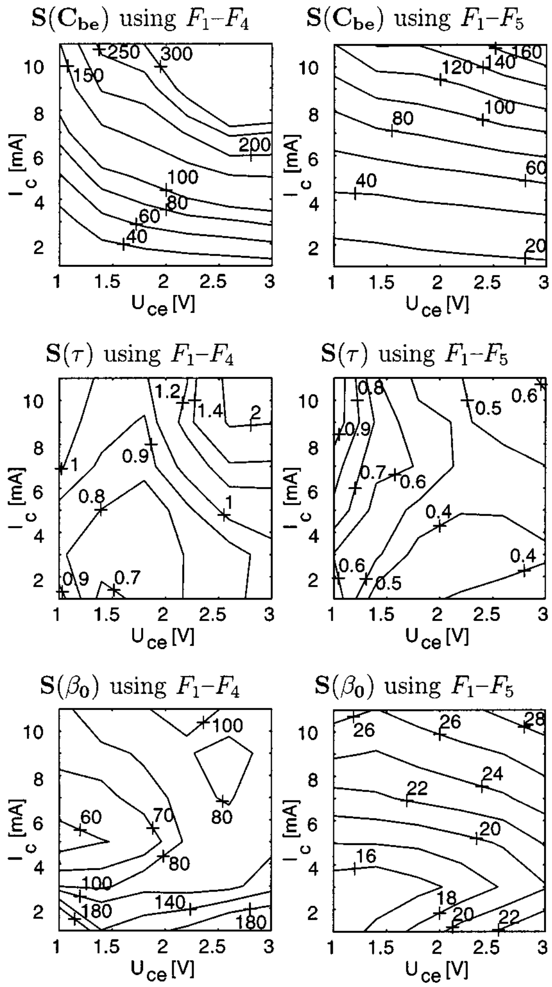

Fig. 4. Bias dependence of the C_{be}, τ, and β_0 insignificances using S-parameters only (F_1–F_4) and using the S-parameters and the current gain term B (F_1–F_5).

V. Conclusions

Several techniques for numerical parameter extraction have been evaluated. The significance of small-signal element values extracted by numerical fitting to measured S-parameters was considerably better than fitting to Z-parameters and was further improved by adding a function that emphasizes the most unreliable elements. The chosen B-function does not need to be the best choice, but it also significantly supports the physical relevance of these elements, thereby improving the usefulness of the extracted model for process monitoring.

References

[1] D. R. Pehlke and D. Pavlidis, "Evaluation of the factors determining HBT high-frequency performance by direct analysis of S-parameter data," *IEEE Trans. Microwave Theory Tech.*, vol. 40, pp. 2367–2373, Dec. 1992.

[2] S. J. Spiegel, D. Ritter, R. A. Hamm, A. Feygenson, and P. R. Smith, "Extraction of the InP/GaInAs heterojunction bipolar transistor small-signal equivalent circuit," *IEEE Trans. Electron Devices*, vol. 42, pp. 1059–1064, June 1995.

[3] J. M. M. Rios, L. M. Lunardi, C. S., and Y. Miyamoto, "A self-consistent method for complete small-signal parameter extraction of InP-based heterojunction bipolar transistors (HBT's)," *IEEE Trans. Microwave Theory Tech.*, vol. 45, pp. 39–44, Jan. 1997.

[4] S. Tiwari, *Compound Semiconductor Device Physics*. New York: Academic, 1992.

[5] S. A. Maas and D. Tait, "Parameter-extraction method for heterojunction bipolar transistors," *IEEE Microwave Guided Wave Lett.*, vol. 2, pp. 502–504, Dec. 1992.

[6] I. Schnyder, M. Rohner, D. Huber, C. Bergamaschi, and H. Jäckel, "A laterally etched collector InP/InGaAs(P) DHBT process for high speed power applications," presented at the Int. Conf. Indium Phosphide and Related Mater., 2000.

Comments on Representation of Surface Leaky Waves on Uniplanar Transmission Lines

Jan Macháč and Ján Zehentner

***Abstract*—This paper compares partial waves approximating a surface leaky wave on a uniplanar transmission line with substrate surface waves supported by its substrate. It is shown that their field distributions and the propagation constants differ. These differences increase with rising leakage constant, and with the growing distance of the corresponding pole of the Green function from the real axis on the spectral variable complex plane. The reported findings are demonstrated on the slotline.**

***Index Terms*—Leaky waves, printed-circuit lines, slotlines.**

I. Introduction

Leaky waves considerably deteriorate the behavior of planar microwave and millimeter-wave circuits and transmission lines due to increased losses, occurrence of crosstalk between neighboring parts of the circuit, and pulse distortion. For these reasons, leaky waves have been intensively studied in recent years [1]–[4]. There are two kinds of leaky waves supported by open planar transmission lines. Surface leaky waves take power away into the dielectric substrate, while space leaky waves radiate into space and may also leak power into the substrate. In this paper, we discuss only surface leaky waves.

There is a general understanding that partly or entirely open planar transmission lines can suffer from loss of transmitted power leaking into the surface leaky waves, which, far away from the line axis, pass on the TM or TE waves supported by the dielectric substrate [1], [2], [5]. A leaky wave can be interpreted as a superposition of two or more nonuniform partial waves propagating at some angle to the line axis, plus the remaining field bound to the line [2], [5], [6]. The propagation constants of these partial waves are assumed to be equal to the propagation constant of the substrate surface wave k_s [5], which is real for a lossless line. Assuming sufficiently weak leakage, when the imaginary part of a leaky-wave propagation constant is negligible in comparison with phase constant β, the angle under which the partial wave propagates is [2], [3]

$$\Theta_\beta = \arccos \frac{\beta}{k_s}. \quad (1)$$

Manuscript received May 25, 1999; revised October 23, 2000. This work was supported by the Grant Agency of the Czech Republic under Project 102/00/0025, and by the Research Programme J04/98 212300014 and Research Programme MSM 216200031.

The authors are with the Faculty of Electrical Engineering, Department of Electromagnetic Field, Czech Technical University, 16627 Prague 6, Czech Republic (e-mail: jmachac@cesnet.cz).

Publisher Item Identifier S 0018-9480(02)01171-7.